Methanol-to-Olefin Process

DOI: 10.1002/anie.200705453

A Complete Catalytic Cycle for Supramolecular Methanol-to-Olefins Conversion by Linking Theory with Experiment**

*David M. McCann, David Lesthaeghe, Philip W. Kletnieks, Darryl R. Guenther, Miranda J. Hayman, Veronique Van Speybroeck, Michel Waroquier, and James F. Haw**

Unraveling the reaction mechanism of extremely complex catalytic processes can be a challenging task from a purely experimental viewpoint. For an industrially important process like the conversion of methanol into olefins (MTO),[1] this is especially the case, as secondary reactions often consume and mask the primary products. Methanol is easily and economically converted into olefins over solid acid zeolite catalysts, yet the ease of MTO conversion is in stark contrast to the difficulty of elucidating the underlying mechanism.[1] Instead of plainly following direct routes,[2–5] the MTO process has been found to proceed through a hydrocarbon pool mechanism, in which organic reaction centers act as co-catalysts inside the zeolite pores, adding a whole new level of complexity to this issue.[6–9] Therefore, a detailed understanding of the elementary reaction steps can best be obtained with the complementary assistance of theoretical modeling. Several experimental observables add to the theoretician's challenge: any full catalytic cycle should not only provide low-energy pathways towards olefin formation, but it should also explain the zeolite-specific product distribution. Furthermore, it should contain the cationic intermediates as observed by in situ NMR spectroscopic methods,[7,10,11] as well as an explanation for the scrambling of labeled carbon atoms into both the hydrocarbon pool species and the olefin products.[7,9,12]

Herein, we report a working catalytic cycle for the conversion of methanol into olefins, in full consistency with both experimental and theoretical observations. For each step, rate constants are presented which were obtained by quantum chemical simulations on a supramolecular model of both the HZSM-5 zeolite and the co-catalytic hydrocarbon pool species (see Methods section). This work not only represents the most robust computational analysis of a successful MTO route to date, but it also succeeds in tying together the many experimental clues.

[*] D. M. McCann, P. W. Kletnieks, D. R. Guenther, M. J. Hayman, Prof. Dr. J. F. Haw
Department of Chemistry, University of Southern California
Los Angeles, CA 90089-1661 (USA)
Fax: (+1) 213-740-0930
E-mail: jhaw@usc.edu

Dr. Ir. D. Lesthaeghe, Prof. Dr. Ir. V. Van Speybroeck, Prof. Dr. M. Waroquier
Center for Molecular Modeling, Ghent University
Proeftuinstraat 86, 9000 Gent (Belgium)

[**] This work is supported by the Fund for Scientific Research, Flanders (FWO) and the Research Board of Ghent University.

Supporting information for this article is available on the WWW under http://www.angewandte.org or from the author.

The first clue towards identification of a successful hydrocarbon pool route is the co-catalytic effect of toluene and higher methylbenzenes.[12] Scrambling of labeled carbon atoms from the methanol feed into these methylbenzenes (as shown in Figure 1) as well as into the olefin products further illustrates the catalytic activity of a methylbenzene pool. Additional clues are provided by in situ NMR spectroscopy,

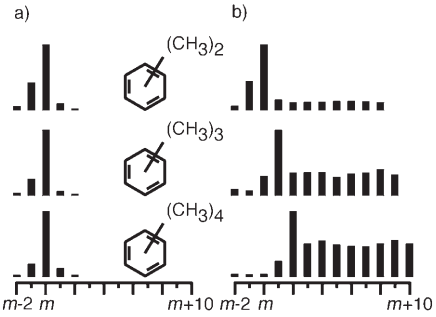

Figure 1. Ion mass distributions for several methylbenzene species from a) the pure ^{12}C compound and b) those generated from a 10 min flow of ^{13}C-methanol and *para*-xylene (mole ratio 20:1) at a methanol weight hourly space velocity of 0.54 over a 300 mg bed of HZSM-5 (Si/Al=40), at 648 K and under 200 sccm flowing helium carrier gas.

with which crucial cationic intermediates can be identified. Specifically within the HZSM-5 zeolite, both a 5-membered ring cation (1,3-dimethylcyclopentadienyl; cation **1**) and a 6-membered ring cation (1,1,2,4,6-pentamethylbenzenium; cation **2**) have been reported.[7,11] Both intermediates are shown in Figure 2. A third important observation is the large variation in product distribution depending on the zeolite catalyst used. For example in HZSM-5, isobutene is abundantly observed (8%) as the third-most-produced hydrocarbon, as illustrated in Figure 3.

These experimental clues are all combined in the theoretically proposed catalytic cycle shown in Figure 4, which is based on the paring mechanism.[13] Gas-phase DFT calculations on similar reactions with only a hydrocarbon pool catalyst (modeling the zeolite as an isolated proton) have been studied earlier by Kolboe et al.[14] These gas-phase calculations show that the production of olefins from benzenium and/or cyclopentenyl cations proceed with larger barriers than any corresponding to

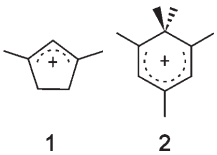

Figure 2. Stable cyclic cations within the HZSM-5 zeolite, as observed with in situ NMR spectroscopy: **1**: 1,3-dimethylcyclopentadienyl cation; **2**: 1,1,2,4,6-pentamethylbenzenium cation.

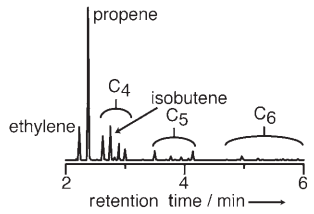

Figure 3. Gas chromatography/flame-ionization detector (GC-FID) chromatogram detailing the light olefins exiting a 300 mg catalyst bed of HZSM-5 (framework Si/Al = 40) following a 10 min flow of methanol at a weight hourly space velocity of 4. The catalyst bed is at 648 K under 200 sccm flowing helium carrier gas.

the observed rapid scrambling of carbon atoms. However, the stabilizing electronic confinement effect of a zeolite framework on these cations acts beneficially towards lowering energy barriers, as earlier demonstrated for the crucial *gem*-methylation steps.[15] A similar favorable effect for the production of olefins is observed here: every step in Figure 4 has been considered with the influence of a full-cage representation of the HZSM-5 zeolite (46T cluster) which has been described in earlier work,[15] as well as its contents. Figure 4 also includes the calculated rate constants for each individual step at 673 K.[16]

Firstly, toluene is linked to the 1,1,2,4,6-pentamethylbenzenium cation (**2**), which occurs through repeated *gem*-methylations of the ring carbons of toluene and subsequent aromatics (steps M1–M4 in Figure 4). The *gem*-methylation of a methylbenzene and production of a higher methylbenzene (steps M1–M3)[17] is performed through a relatively slow methylation step, followed by a much faster deprotonation step:

1. The methyl group of methanol is transferred towards a ring carbon atom with simultaneous transfer of the acid-site proton to the oxygen of methanol. An intermediate benzenium cation and water are formed.
2. Regeneration of a neutral aromatic is achieved by rapid abstraction of a proton from the polymethylated benzenium cation.

These two steps illustrate a full *gem*-methylation cycle and are subsequently performed for every aromatic built, until 1,2,3,5-tetramethylbenzene is reached. The 1,1,2,4,6-pentamethylbenzenium cation (**2**) is consequently formed by a similar methylation step, yet this time on an already substituted ring carbon atom. This methylation (step M4) ignites the second half of the cycle,[15] in which no further methylations occur and the hydrocarbon pool species undergoes various intramolecular rearrangements (steps I1–I3, Figure 4). These rearrangements include the formation of isobutene in HZSM-5.

In this second part of Figure 4, the intramolecular isomerizations I1–I3 allow the 1,1,2,4,6,-pentamethylbenzenium

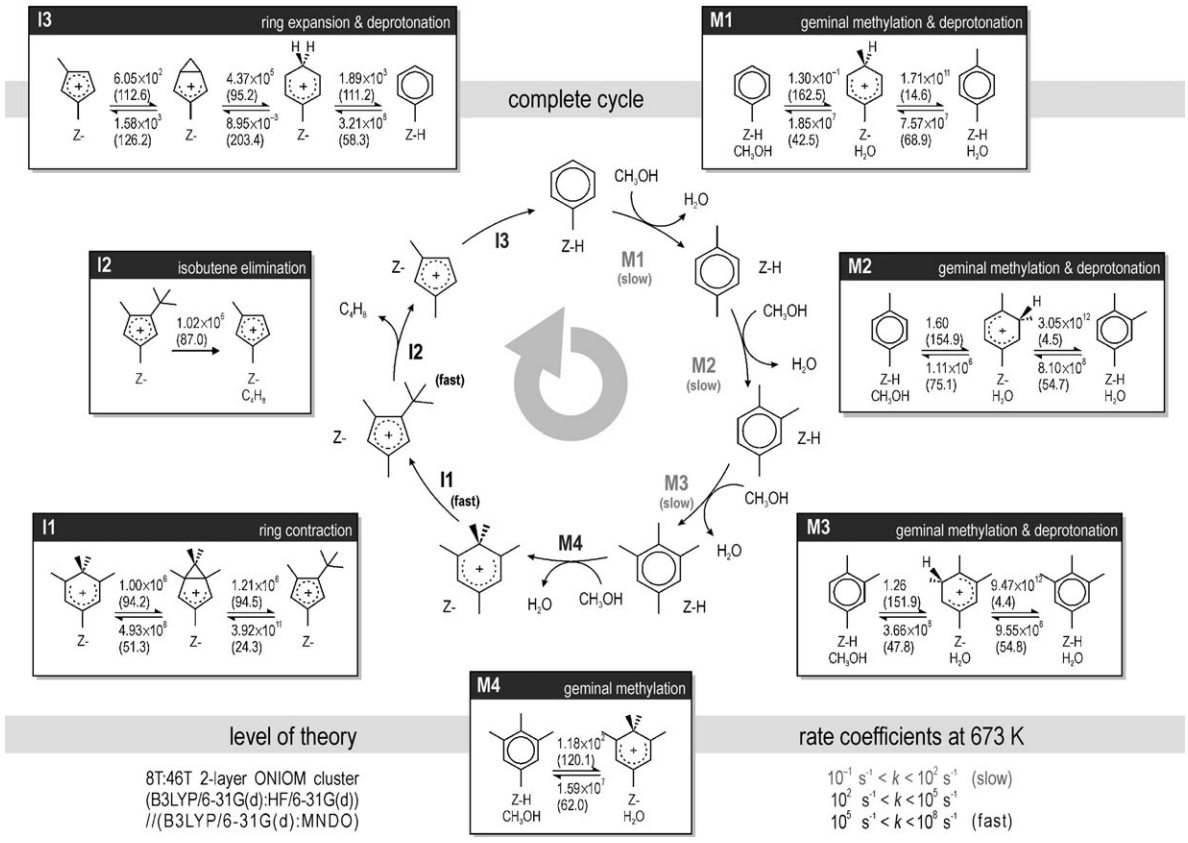

Figure 4. Full catalytic cycle for carbon-atom scrambling and isobutene formation from methanol through a combined methylbenzene/cyclopentenyl cation pool in HZSM-5. Calculated rate constants at 673 K are given in s^{-1} and reaction barriers at 0 K (in brackets) are given in kJ mol^{-1}; for details see text.

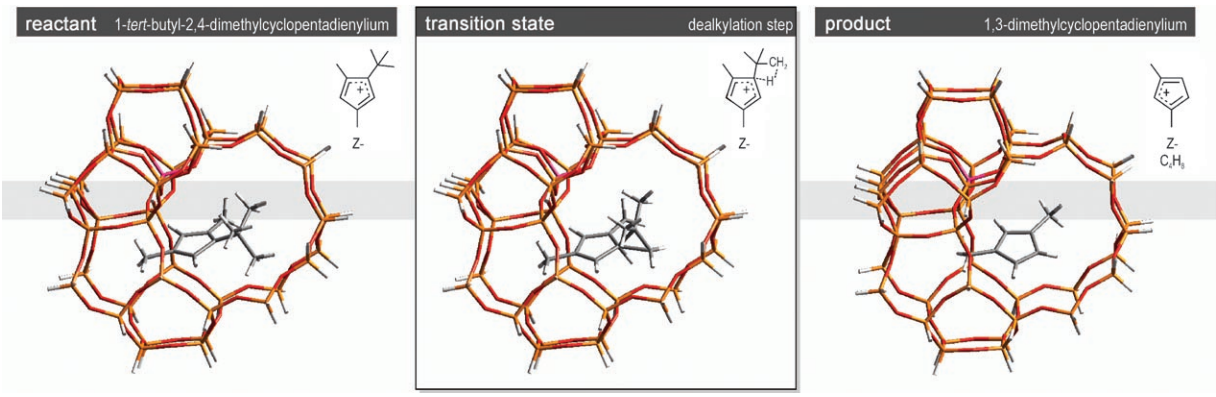

Figure 5. Stationary points in the 46T cluster for splitting off isobutene from the 1-*tert*-butyl-2,4-dimethylcyclopentadienylium cation (step I2). Isobutene successfully exits the HZSM-5 channels as a major product.

cation (**2**) not only to split off isobutene, but also to simultaneously scramble carbon atoms:

I1. A 6→5 carbon atom contraction of the benzene ring forming a 1,3,5,6,6-pentamethylbicyclo[3.1.0]hexenyl cation is the first step. A shift of a bridgehead methyl group while simultaneously breaking the three-membered carbon ring results in formation of 1-*tert*-butyl-2,4-dimethylcyclopentadienylium cation.

I2. The formation of the *tert*-butyl group allows for isobutene to be produced. Upon removal of isobutene, the 1,3-dimethylcyclopentadienylium cation is formed, which is similar in carbon backbone structure to the observed 1,3-dimethylcyclopentadienyl cation (**1**). The stationary points for removal of the *tert*-butyl group are shown in Figure 5.

I3. This cation is then expanded to toluene to close the cycle and complete the scheme. Furthermore, this expansion results in the incorporation of a methyl carbon into the ring, explaining the scrambling as observed in Figure 1. The expansion process proceeds in three steps: the transfer of a hydrogen atom to the cyclopentyl ring and shift of the methyl carbon to form a 3-methylbicyclo-[3.1.0]hexenyl cation, followed by the expansion of the three-membered ring and finally the deprotonation to toluene. The unexpected low barrier and high rate coefficient for the reverse reaction (protonation of toluene) is created by the toluene product being caught in the sinusoidal channel after the transition state. This results in a both energetically and entropically unfavored position, which is why the toluene molecule is expected to migrate to a lower-lying minimum at the channel intersections from which the catalytic cycle can resume in step M1.

When modeled in the gas-phase, the intramolecular rearrangements leading to removal of an alkyl substituent and incorporation of methyl carbon atoms into the ring are very energy demanding. However, including the full-cage model significantly increases the rate constants, rendering the steps I1–I3 several orders of magnitude faster than the familiar methylation reactions M1–M3. Furthermore, these rate coefficients are also much higher than those for direct methanol conversion, which are typically around $10^{-6}\,s^{-1}$ at 720 K.[3] However, reverse rates are often high as well, which means that even though this is a successful catalytic cycle, it cannot be the only one operating. As the cavities often contain more hexa- and pentamethylbenzene, additional cycles which are linked to this particular one (starting from higher methylbenzenes rather than toluene) will have to operate through even faster routes to account for the ethene/propene production.

This catalytic cycle is unique, as it connects toluene to the 1,1,2,4,6-pentamethylbenzenium cation (**2**), the largest cation seen experimentally in HZSM-5, as well as to the 1,3-dimethylcyclopentadienylium cation (**1**). These cations are stabilized by the electronic confinement effect and can only be adequately described with a full surrounding framework. The experimental observation of multiple scrambling would be achieved by repeated iterations through this scheme, resulting in both labeling of the olefins and of the aromatics. Furthermore, this cycle does not only explain the observed cations as well as the scrambling, but it also provides a plausible route for the formation of isobutene from methanol as a major product in HZSM-5. Quite strikingly, this is the first complete route for any type of MTO conversion containing not a single major bottleneck.

Work performed here has greatly enhanced previous research and developed a fundamental understanding of the actual steps involved to produce olefins from aromatic reaction centers. However, other hydrocarbon pool species might also be stable within the pores of the zeolite and these could result in various other major olefin products like ethylene and propene. Furthermore, the expansion of this work to other common MTO zeolites and possibly to the chabazite topology aluminophosphate HSAPO-34 would be beneficial, as different topologies and different compositions will most likely lead to different major catalytic cycles.

Methods

Optimizations of the 46T clusters have been performed at the ONIOM(B3LYP/6-31G(d):MNDO) level using the Gaussian03 package.[18] The high DFT level was used for an embedded 8T-cluster, which includes the acid site, and the organic guest molecules. The 46T

cluster was saturated with hydrogen atoms. Only these saturating hydrogen atoms were fixed to prevent collapse of the cage. All other low-level framework atoms were allowed to fully reposition themselves to host the large incorporated species. Inclusion of the full cage was necessary, as electrostatic interactions and shape selectivity greatly influence reaction barriers, which is especially pronounced in ZSM-5.[15] Frequency calculations were performed on all, ensuring stability and the identification of proper transition states. Single point energies have been corrected by using the ONIOM(B3LYP/6-31G(d):HF/6-31G(d)) level of theory. This method does not provide an optimal treatment of the van der Waals interactions. Even newly developed strategies to address this issue cannot be routinely applied to hydrocarbon reactions in zeolites yet because of the system's size.[19] The rate constants were obtained through unimolecular transition state theory, in which the entire supramolecular complex (cage+contents) was handled as a single molecule. This approach results in rate constants which are smaller than experimentally obtained rate constants for isobutene formation, but within similar orders of magnitude.

Received: November 28, 2007
Revised: February 13, 2008
Published online: April 28, 2008

Keywords: cationic aromatics · geminal methylation · hydrocarbon pool · methanol-to-olefins process · zeolites

[1] M. Stocker, *Microporous Mesoporous Mater.* **1999**, *29*, 3 – 48.
[2] W. G. Song, D. M. Marcus, H. Fu, J. O. Ehresmann, J. F. Haw, *J. Am. Chem. Soc.* **2002**, *124*, 3844 – 3845.
[3] D. Lesthaeghe, V. Van Speybroeck, G. B. Marin, M. Waroquier, *Angew. Chem.* **2006**, *118*, 1746 – 1751; *Angew. Chem. Int. Ed.* **2006**, *45*, 1714 – 1719.
[4] D. M. Marcus, K. A. McLachlan, M. A. Wildman, J. O. Ehresmann, P. W. Kletnieks, J. F. Haw, *Angew. Chem.* **2006**, *118*, 3205 – 3208; *Angew. Chem. Int. Ed.* **2006**, *45*, 3133 – 3136.
[5] Z. M. Cui, Q. Liu, W. G. Song, L. J. Wan, *Angew. Chem.* **2006**, *118*, 6662 – 6665; *Angew. Chem. Int. Ed.* **2006**, *45*, 6512 – 6515.
[6] R. M. Dessau, *J. Catal.* **1986**, *99*, 111 – 116.
[7] A. Sassi, M. A. Wildman, H. J. Ahn, P. Prasad, J. B. Nicholas, J. F. Haw, *J. Phys. Chem. B* **2002**, *106*, 2294 – 2303.
[8] J. F. Haw, W. G. Song, D. M. Marcus, J. B. Nicholas, *Acc. Chem. Res.* **2003**, *36*, 317 – 326.
[9] a) I. M. Dahl, S. Kolboe, *Catal. Lett.* **1993**, *20*, 329 – 336; b) I. M. Dahl, S. Kolboe, *J. Catal.* **1994**, *149*, 458 – 464; c) I. M. Dahl, S. Kolboe, *J. Catal.* **1996**, *161*, 304 – 309.
[10] a) T. Xu, J. F. Haw, *Top. Catal.* **1997**, *4*, 109 – 118; b) E. J. Munson, D. B. Ferguson, A. A. Kheir, J. F. Haw, *J. Catal.* **1992**, *136*, 504 – 509.
[11] a) J. F. Haw, J. B. Nicholas, W. Song, F. Deng, Z. Wang, T. Xu, C. S. Heneghan, *J. Am. Chem. Soc.* **2000**, *122*, 4763 – 4775; b) T. Xu, D. H. Barich, P. W. Goguen, W. G. Song, Z. K. Wang, J. B. Nicholas, J. F. Haw, *J. Am. Chem. Soc.* **1998**, *120*, 4025 – 4026.
[12] a) R. M. Dessau, R. B. LaPierre, *J. Catal.* **1982**, *78*, 136 – 141; b) T. Mole, G. Bett, D. Seddon, *J. Catal.* **1983**, *84*, 435 – 445; c) O. Mikkelsen, P. O. Rønning, S. Kolboe, *Microporous Mesoporous Mater.* **2000**, *40*, 95 – 113; d) B. Arstad, S. Kolboe, *J. Am. Chem. Soc.* **2001**, *123*, 8137 – 8138; e) M. Bjørgen, U. Olsby, D. Petersen, S. Kolboe, *J. Catal.* **2004**, *221*, 1 – 10; f) S. Svelle, F. Joensen, J. Nerlov, U. Olsbye, K.-P. Lillerud, S. Kolboe, M. J. Bjørgen, *J. Am. Chem. Soc.* **2006**, *128*, 14770 – 14771; g) W. Song, H. Fu, J. F. Haw, *J. Phys. Chem. B* **2001**, *105*, 12839 – 12843; h) H. Fu, W. Song, D. M. Marcus, J. F. Haw, *J. Phys. Chem. B* **2002**, *106*, 5648 – 5652.
[13] C. J. Egan, G. E. Langlois, R. J. White, *J. Am. Chem. Soc.* **1962**, *84*, 1204 – 1212.
[14] a) B. Arstad, S. Kolboe, O. Swang, *J. Phys. Org. Chem.* **2004**, *17*, 1023 – 1032; b) B. Arstad, S. Kolboe, O. Swang, *J. Phys. Chem. A* **2005**, *109*, 8914 –8922.
[15] D. Lesthaeghe, B. De Sterck, V. Van Speybroeck, G. B. Marin, M. Waroquier, *Angew. Chem.* **2007**, *119*, 1333 – 1336; *Angew. Chem. Int. Ed.* **2007**, *46*, 1311 – 1314.
[16] A reverse rate constant for splitting off isobutene is not included as optimization showed the isobutene product to successfully exit the zeolite catalyst.
[17] A. M. Vos, X. Rozanska, R. A. Schoonheydt, R. A. van Santen, F. Hutschka, J. Hafner, *J. Am. Chem. Soc.* **2001**, *123*, 2799 – 2809.
[18] Gaussian 03 (Revisions C.02 and D.01), M. J. Frisch et al., see the Supporting Information.
[19] C. Tuma, J. Sauer, *Phys. Chem. Chem. Phys.* **2006**, *8*, 3955 – 3965.

